

Article

Effect of Ultrasonic Degassing on Mg-Ca Binary Alloy by Ultrasonic Treatment

Zheng Jia *, Bing Yu and Li Fu

College of Mechanical Engineering, Shenyang University, Shenyang 110044, China

* Correspondence: jz140@syu.edu.cn

Abstract: The effect of ultrasonic treatment parameters, including ultrasonic treatment duration, frequency resonance, and treatment temperature, on the degassing of Mg-3.03Ca alloys was investigated. The results indicated that the optimum degassing efficiency could be obtained under the ultrasonic resonant condition. When applying ultrasonic treatment for 90 s with 150 W at 700 °C, the minimum hydrogen content and the highest degassing efficiency are obtained, respectively (42.8 cm³/100 g and 27.5%). The ultrasonic treatment can remove the gas from the melt and refine the microstructures. Finally, the mechanism of ultrasonic degassing and refinement was analyzed.

Keywords: ultrasonic treatment; Mg-3.03Ca alloy; hydrogen content; grain refinement; cavitation effect



Citation: Jia, Z.; Yu, B.; Fu, L. Effect of Ultrasonic Degassing on Mg-Ca Binary Alloy by Ultrasonic Treatment. *Crystals* **2022**, *12*, 1162. <https://doi.org/10.3390/cryst12081162>

Academic Editors: Xingrui Chen, Weitao Jia, Xuan Liu, Qiyang Tan and Pavel Lukáč

Received: 28 July 2022

Accepted: 17 August 2022

Published: 18 August 2022

Publisher's Note: MDPI stays neutral with regard to jurisdictional claims in published maps and institutional affiliations.



Copyright: © 2022 by the authors. Licensee MDPI, Basel, Switzerland. This article is an open access article distributed under the terms and conditions of the Creative Commons Attribution (CC BY) license (<https://creativecommons.org/licenses/by/4.0/>).

1. Introduction

Magnesium alloys have a series of advantages, such as low density, high specific strength, high stiffness, good damping performance, high thermal conductivity, and low cost [1–3]. Therefore, magnesium alloys are widely used in the automobile, communication, and electronics industry [4,5]. It is predicted that magnesium alloys will become one of the most important lightweight and high-strength materials in the 21st century.

Casting is a common method of processing magnesium alloys [6,7]. However, magnesium alloys usually absorb large amounts of hydrogen during the melting process [8,9]. Hydrogen is generated by the reaction between water vapor from the air, the melt, and the moist flux. For example, the hydrogen solubility is about 30 mL/100 g in magnesium alloys that melt at 730 °C [10]. If hydrogen is dissolved into the solid metal, the hydrogen will become the strengthening element. However, once the hydrogen content exceeds the solid solution limitation, the second phase changes to bubbles. The hydrogen can enhance the formation of the porosity and severely deteriorate the properties of the magnesium alloys. Therefore, the removal of the hydrogen from the melt is very important. However, research papers on this issue are still rare up to now.

High-energy ultrasonic has a unique acoustic effect [11–13]. If the ultrasonic vibration is applied for a proper time during the solidification, the structure of the casting ingot will change from coarse columnar grains to uniform and fine equiaxed grains [14]. The macro- and micro-segregation of the casting ingot will be improved. Moreover, ultrasonic can effectively remove the gas from the melt, thereby improving the density of the ingot. At present, the degassing problem mainly focuses on aluminum alloy. However, the degassing problem of magnesium alloy is currently ignored. In fact, according to the above, the degassing of magnesium alloys is also very important. For magnesium alloys, the traditional degassing methods mainly include vacuum treatments, inert gas blowing, chlorine additions, rare earth additions, and so on. The ultrasonic degassing of the melt is also reported in some of the literature [15–18]. For example, in the Soviet Union [19], some researchers found that the mechanism of ultrasonic degassing was intimately attributed to cavitation, which depends on ultrasonic power. Increasing the ultrasonic power could improve the degassing effect. It was reported by the researchers of the Oak Ridge National Laboratory that the ultrasonic degassing efficiency of the A356 alloy melt was related to

the ultrasonic treating temperature or time [20,21]. The results indicated that increasing either the temperature or the treating time could improve the degassing effect. Recently, Wu et al. [22,23] considered that the degassing effect on the melt or the semi-solid slurry aluminum alloys should be attributed to a combination of cavitation and acoustic streaming, which is related to ultrasonic power. Up to now, little research has been done on the degassing of magnesium alloys melted by ultrasonic. Therefore, the effects of the ultrasonic treatment duration, ultrasonic resonant, and treatment temperature on the degassing effect and solidification structure of the Mg-3.03Ca alloy were studied for this paper, and the mechanism of ultrasonic degassing and refining are also discussed.

2. Experimental Methods

Figure 1 is a schematic diagram of an ultrasonic device. The ultrasonic system used in the experiment mainly includes an ultrasonic generator with a frequency of 20 ± 2 kHz, a piezoelectric ceramic transducer, an acoustic transmitter, an air-cooling system, and a temperature control system. The power of the ultrasonic generator is continuously adjustable from 0~150 W. The temperature of the melt and the preheating temperature of the ultrasonic transmitter are controlled by the temperature control system.

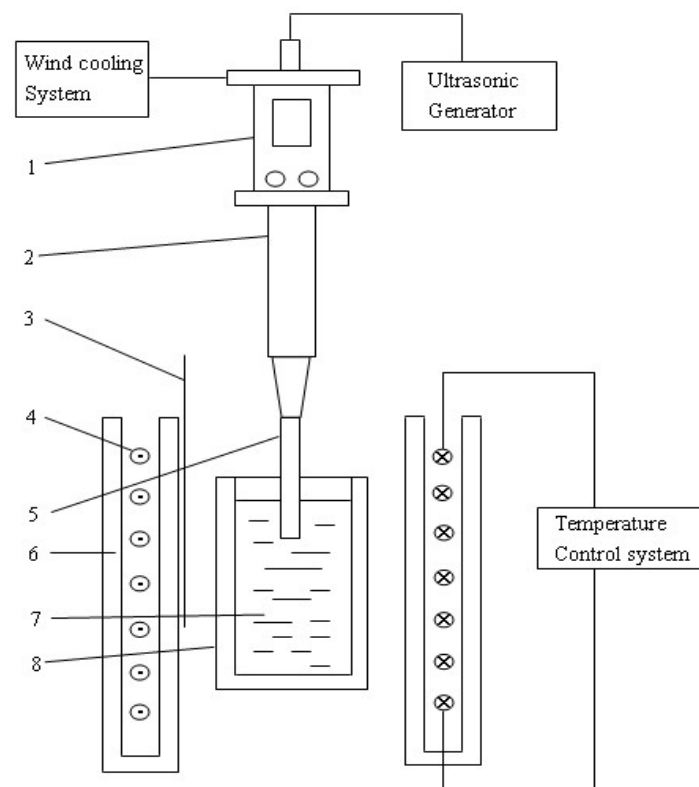


Figure 1. Schematic diagram of the ultrasonic treatment experimental set-up. 1—Ultrasonic transducer; 2—Cone; 3—Thermocouple; 4—Resistance heater; 5—Ultrasonic radiator; 6—Ceramic tube; 7—Mg-3.03Ca alloy melt; 8—The iron crucible.

The alloy of Mg-3.03Ca (the mass fraction is the same below) is prepared by melting magnesium of 99.9% and 99.99% calcium. The alloy was put into a self-made iron crucible and smelted in the resistance furnace. The mixed gas of $\text{CO}_2 + 0.5\%\text{SF}_6$ was used to prevent the oxidation and combustion of the magnesium alloy during smelting. The alloy was heated to 740°C to melt completely and was held for 10 min after reduction of the required temperature. At the same time, the preheated ultrasonic probe (the preheating temperature is the same as the temperature to be processed) was quickly introduced from the top of the crucible into 20 mm, the selected ultrasonic power was 150 W, the processing time was, 30, 60, 90, and 120 s, respectively, the panel of the tuning indicator was changed from 0 to

0.4, and the processing temperature was 730, 700, and 670 °C, respectively. The melt was absorbed by a quartz tube (tested by an RH404 hydrogen gauge), and the microstructure and porosity were observed by a Leica DMR metallography microscope. Therefore, the hydrogen content was measured by the solid state.

The degassing efficiency was used as follows:

$$\eta = \frac{C_0 - C}{C_0} \quad (1)$$

where

η —is the degassing efficiency;

C_0 —is the initial hydrogen content in melt;

C —is the hydrogen content in the melt after degassing.

3. Results and Discussion

3.1. Effect of Ultrasonic Treatment Duration on Hydrogen Content and Refinement of Mg-3.03Ca Alloy

Figure 2 shows the effect of the ultrasonic treatment duration on the hydrogen content by 150 W at 700 °C. The hydrogen content was 59 cm³/100 g without the ultrasonic treatment. With the increase in the ultrasonic processing time, the hydrogen content can reach the minimum value (42.8 cm³/100 g) at 90 s. The hydrogen content slightly increased at a processing time of 120 s (43.5 cm³/100 g).

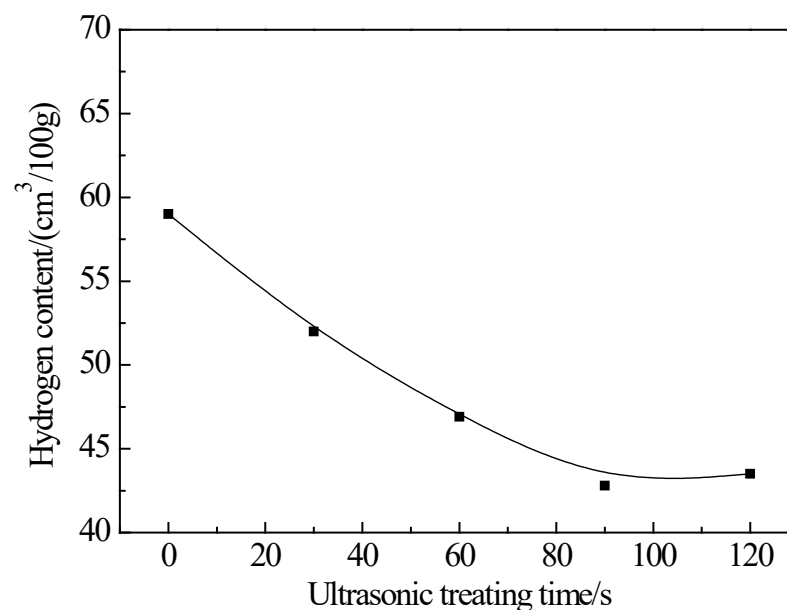


Figure 2. Effect of ultrasonic treating duration on hydrogen content of Mg-3.03Ca alloy.

Without the ultrasonic treatment, the microstructure of the alloy has lots of coarse dendrites, and there are more porosities between the dendrites, which is with a large amount in the untreated ingots. After the ultrasonic treatment for 30 s, there exist lots of porosities and dendrites, as shown in Figure 3b. When the ultrasonic treatment duration is 60 s, the grains are rounded and refined, but there are still some pores. Subsequently, when the treatment time increases to 90 s, the grain refinement is very obvious, and the porosity defects in the center of the ingot casting are rarely observed, as shown in Figure 3d. As the treatment time increases to 120 s, the grains are coarsened and nonuniform, as shown in Figure 3e.

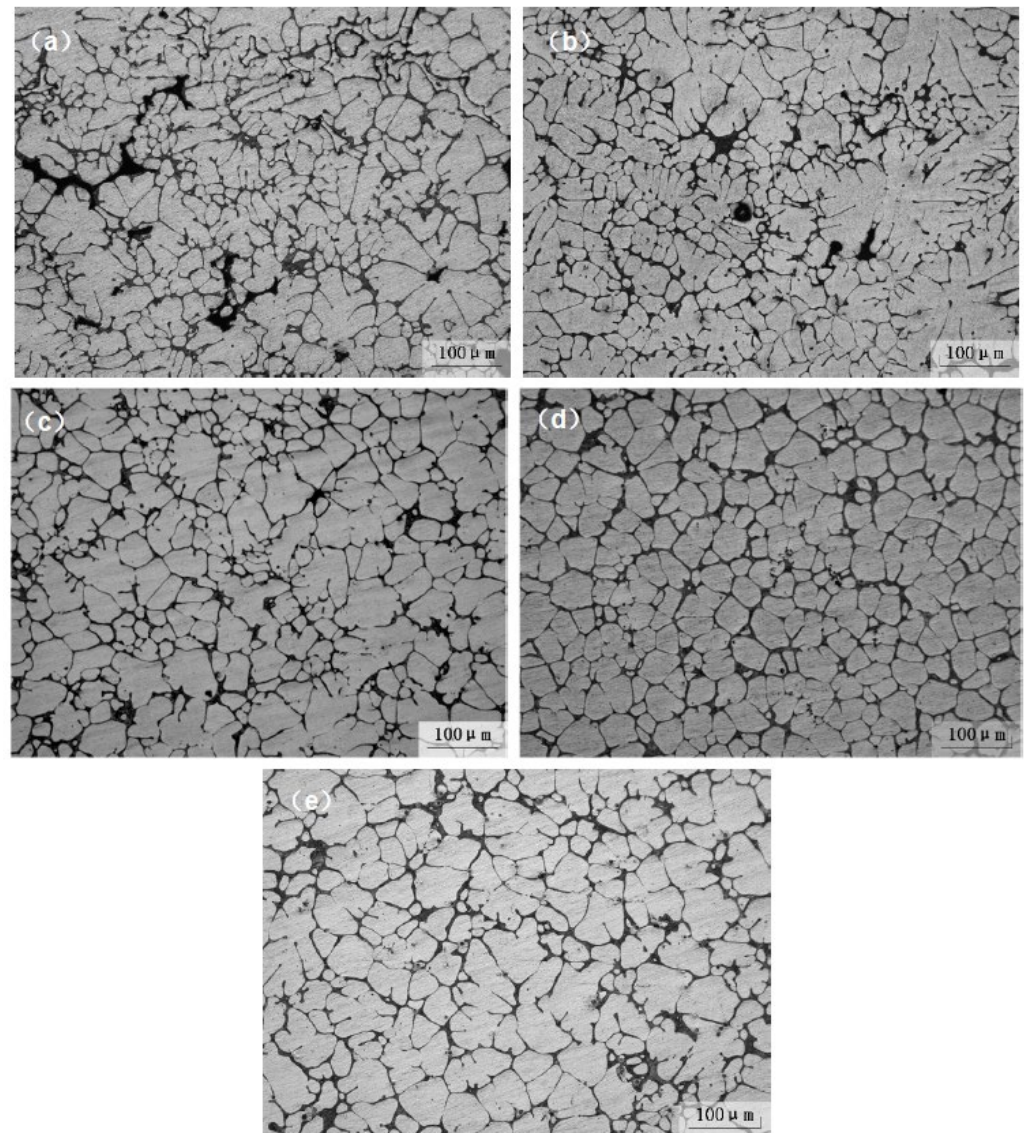


Figure 3. Microstructures of Mg-3.03Ca alloy treated with different ultrasonic treating durations. (a) 0 s; (b) 30 s; (c) 60 s; (d) 90 s; (e) 120 s.

According to G. I. Eskin [10], when the ultrasonic vibration intensity I is lower than a certain power value, it is in the stage of the sub-cavitation effect. When the value exceeds this value, it is considered to be in the development/developed stage of the cavitation effect. The characteristics of these two stages are obviously different, which are described below respectively. The ultrasonic frequency used in this experiment is 20 kHz. It is assumed that the relationship in the smaller range from 20 kHz to 200 kHz is a linear relationship, then the minimum intensity of the cavitation effect is $I_{\min} = 1.25 \times 10^4 \text{ W/m}^2$. It is assumed that all the ultrasonic energy in the experiment is transmitted to the liquid level of the metal melt, and the crucible size diameter is $\varphi = 0.07 \text{ m}$, according to $P = IS$, when $P = 150 \text{ W}$ and the vibration intensity $I = 3.9 \times 10^4 \text{ W/m}^2 > I_{\min}$. It is considered that the melt is at the stage of the developing/developed cavitation effect. In this state, the growth of cavitation bubbles is extremely active, and the significant decrease in the pressure within the bubble leads to the continuous combination and growth of various bubbles, which surface towards the melt to achieve the purpose of degassing. The development/developed stages of the cavitation effect are shown in Figure 4b.

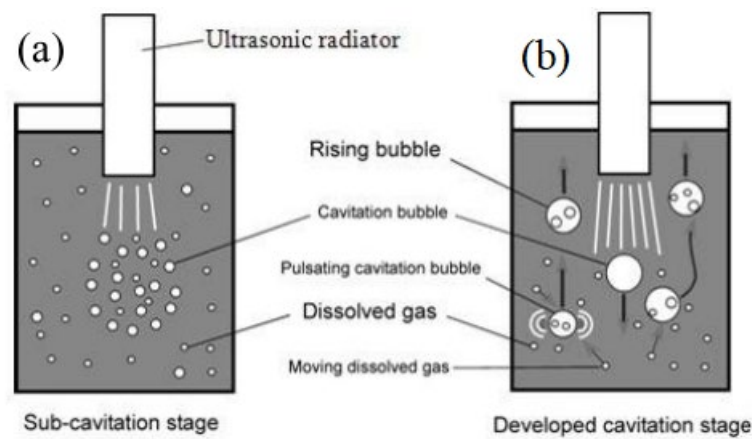


Figure 4. Two different cavitation stages. (a) Sub-cavitation stage; (b) developing/developed cavitation stage.

When the appropriate ultrasonic treatment time is applied to the melt, a large number of cavitation bubbles are generated in the melt. At this moment, if the cavitation bubbles generated in the melt and the ultrasonic frequency are in a resonance relationship, then the cavitation bubbles will grow significantly, and the resonance frequency of the cavitation bubbles can be calculated by the following formula [11]:

$$f = \frac{1}{\pi d} \sqrt{\frac{3kp_0}{\rho_L}} \quad (2)$$

where f is the frequency of the ultrasonic transducer, kHz; d is the diameter of the bubble, m; k is the ratio of the specific heat at a constant pressure to the specific heat at a constant volume of the gas in the bubble, namely $k = \frac{c_p}{c_v}$; p_0 is the hydraulic pressure of the melt, Pa; ρ_L is the density of the pure magnesium melt, kg/m³.

In this experiment, $f = 20$ kHz, $p_0 = 1.01325 \times 10^5$ Pa (1 atm), $k = 1.14$, $\rho_L = 1.577 \times 10^3$ kg/m³ (700 °C), and $d = 2.36 \times 10^{-4}$ m.

Assuming that the cavitation bubble is a sphere with an initial radius of $R_0 = \frac{d}{2}$ and that the floating speed is v and the dynamic viscosity is η , according to the Stokes formula, we have:

$$v = \frac{2gR_0^2(\rho_L - \rho_0)}{9\eta} \quad (3)$$

where ρ_0 is the density of the cavitation bubbles (kg/m³), g is the acceleration of gravity (m/s²), and the viscosity coefficient of the magnesium melt is 1.12×10^{-3} N·s/m² (at 700 °C), so the floating speed of the bubble can be obtained ($v = 0.043$ m/s). The melting depth of the crucible is $H = 0.09$ m. Then, the floating time of the bubble is $t = \frac{H}{v} = 2.09$ s. However, in fact, cavitation bubbles also exist in areas with a depth less than H , and the cavitation bubbles continually combine and grow until they escape from the liquid. The active bubbles make the bubble radius larger than the initial radius. Therefore, it is considered that the bubble float time in the magnesium melt is 2.09 s. Therefore, proper ultrasonic treatment duration (90 s) can effectively remove hydrogen from the melt.

The refining effect produced by the ultrasonic can be explained as follows: When ultrasonic is used to treat the Mg-3.03Ca alloy melt, liquid molecules are subjected to a periodic alternating sound field, and the liquid is subjected to negative pressure and is forced to crack, resulting in cavitation bubbles. Under the motion of the positive phase of the subsequent sound waves, the cavitation bubbles are generated close to or collapse at a very high speed, which locally produces an instantaneous high pressure, high temperature, and strong shock waves within the melt. In the process of the cavitation bubble formation and growth, heat will be absorbed from the surrounding area, which leads to a decrease in the temperature of the metal melt in the area of the cavitation bubble surface, resulting in

local supercooling. However, in the collapse process of the cavitation bubble, the strong shock wave will shatter the primary crystal and the growth, making them into broken crystal particles. The local heat pulse formed by the cavitation constantly impinges on the solidification front and causes local erosion of the interface. The high temperature caused by the cavitation causes the dendrite to melt and also increases the nucleation number, thus increasing the number of grains. When the pressure value exceeds 10^4 MPa, the transition from liquid to solid can be realized. The high pressure generated by ultrasonic processing exceeds this value so that acoustic cavitation can promote the formation of a crystal nucleus. Therefore, the ultrasonic-treated alloy can make the grain fine and even under the effect of acoustic cavitation and acoustic flow. The ultrasonic processing melt occurs when the energy is absorbed by the melt into thermal energy dissipation; the longer the processing time is, the greater the thermal effect is apparent, which causes a prolonged crystal growth time. Therefore, grain coarsening will appear.

3.2. Effect of Ultrasonic Resonance and Non-Resonance on Hydrogen Content and Degassing Efficiency of Mg-3.03Ca Alloy

The ultrasonic generator was adjusted to the resonance before each experiment, and it was regarded as a resonant when the panel of the tuning indicator was changed from 0 to 0.4. Figure 5 shows the degassing efficiency of the Mg-3.03Ca alloy with different degassing processes (the resonance and non-resonance under the ultrasonic power of 150 W for 90 s at 700 °C).

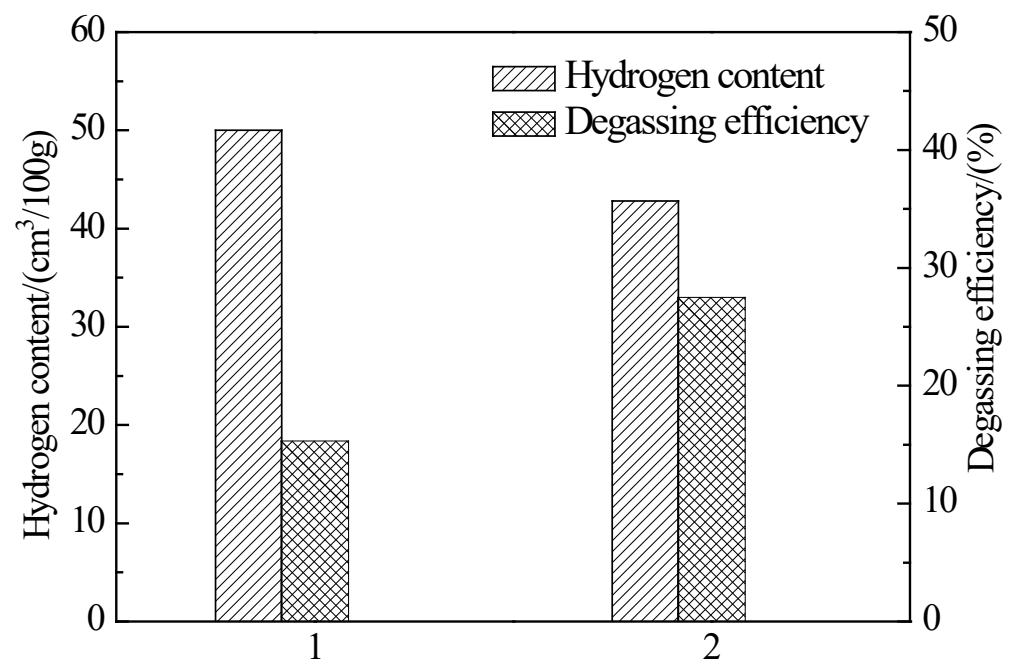


Figure 5. Effect of ultrasonic resonance and non-resonance on the degassing efficiency of Mg-3.03Ca alloy. 1—Non-resonance 2—Resonance.

It can be seen that the Mg-3.03Ca alloy has the best degassing effect under ultrasonic resonance. This phenomenon can be understood in Figure 6 [11]. The cavitation bubbles generated under the ultrasonic resonance can be divided into an expansion stage and a compression stage. The cavitating bubble grows slowly in the expansion stage, and the surface area increases. Meanwhile, the thickness of the diffusion layer also decreases, and the gas concentration increases, which increases the gas concentration gradient in the cavitation bubble and accelerates the moving rate of the gas from the melt into the cavitation bubble. In the compression stage, the cavitation bubble grows rapidly, and the surface area decreases. At this time, the thickness of the diffusion layer will also increase, and the gas concentration will decrease, which will reduce the gas concentration gradient

in the cavitation bubble, so the moving rate of the gas will also decrease. When the melt is in the ultrasonic vibration resonance, the pulsating diffusion movement caused by the continuous expansion and compression of the cavitation bubbles is active. Therefore, the degassing effect is the best under the condition of ultrasonic resonance.

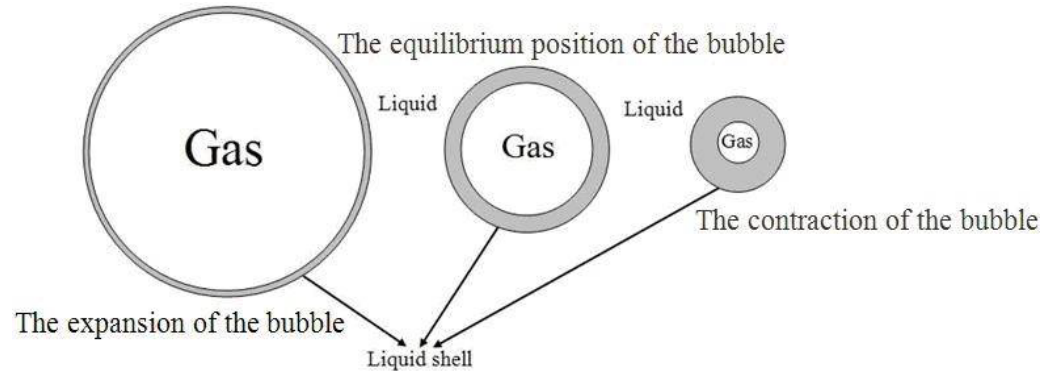


Figure 6. Schematic diagram of the cavitation bubble pulsation.

3.3. Ultrasonic Degassing and Refinement at Different Temperatures

The effect of the ultrasonic treatment temperature at 150 W for 90 s on the degassing was investigated in Figure 7. The maximum degassing efficiency can reach 27.5%, which is higher than those of 730 °C and 670 °C, respectively.

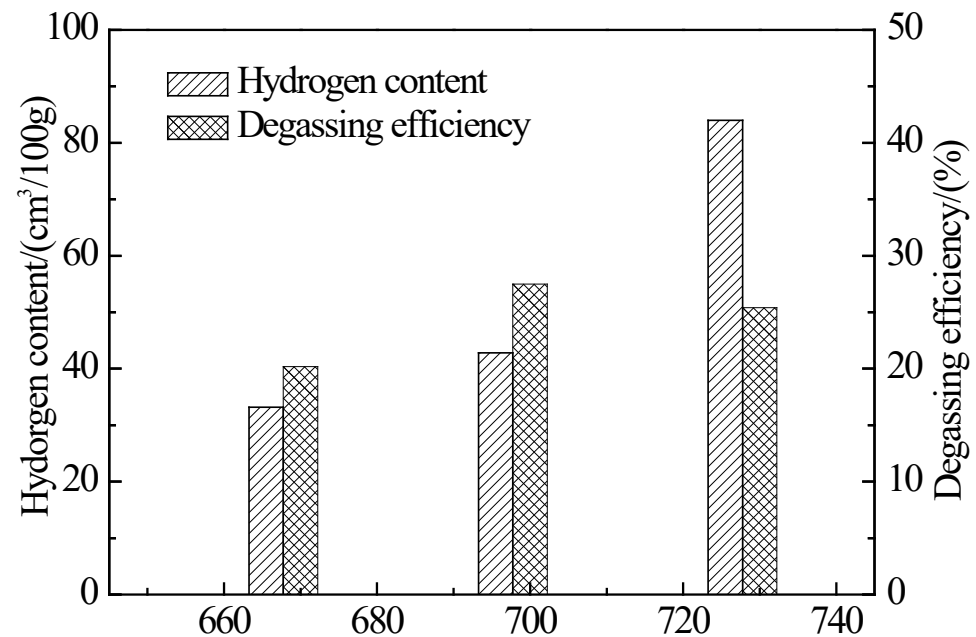


Figure 7. The effect of the ultrasonic treating temperature on the hydrogen content and degassing efficiency of Mg-3.03Ca alloy.

Figure 8 shows the microstructures of the alloy at different temperatures by ultrasonic treatment. Many poles exist in the ingot without the ultrasonic treatment. The microstructures of the ingots at the treatment temperatures of 730 °C and 700 °C show small equiaxed grains. However, the microstructures of the ingots at the treatment temperature of 670 °C show non-uniform grains and lots of pores.

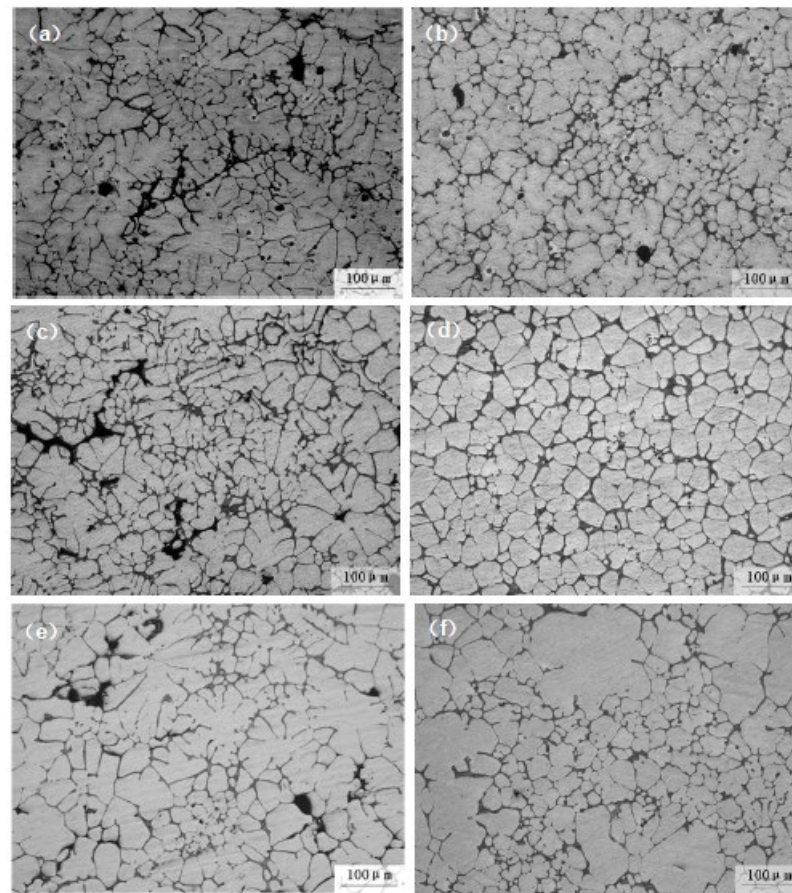


Figure 8. Microstructures of the Mg-3.03Ca alloy treated with different ultrasonic treating temperatures. (a,c,e) without ultrasonic; (b,d,f) ultrasonic treatment (a,b) 730 °C; (c,d) 700 °C; (e,f) 670 °C.

With the increase of the temperature, the hydrogen content of the magnesium melt increases. When the treatment temperature is higher (730 °C), it takes a longer time to remove the gas from the melt. Therefore, 90 s is not enough to completely remove the gas in the melt, with many pores existing and the degassing efficiency decreasing. When the alloy was treated at a low temperature (670 °C), the degassing time of 90 s at this temperature was long because the alloy absorbed less gas than at 730 °C, and a long time of ultrasonic treatment would cause a large number of cavitation bubbles in the melt to distribute uniformly in the melt. In addition, the lower melt temperature makes the melt viscosity larger, which is not beneficial to bubble floating. Therefore, these bubbles remained in the ingot with the temperature decreasing, resulting in a degassing efficiency lower than 730 °C.

It can also be seen from Figure 8 that 90 s treated at 700 °C not only results in the most obvious degassing effect but also makes the grains smaller than those at 730 °C and 670 °C. The reasons for the refinement caused by ultrasonic treatment at different temperatures can be explained as follows: The cavitation effect by ultrasonic is closely related to the treatment temperature of the ultrasonic. If the melt temperature is too high and the cooling rate is slow, crystal nucleation becomes difficult, and then the solidification structure of the alloy is coarse. Meanwhile, the rising of the temperature caused by the thermal effect generated by the ultrasonic will increase the pressure inside the cavitation bubble, which will weaken the cavitation effect and make the refining effect not obvious. If the temperature is too low and the melt viscosity is greater, the cavitation and acoustic effect will be weakened, so the ultrasonic treatment at a lower temperature cannot achieve the refinement and degassing effect.

The solidification structure of the ingot becomes fine and uniform by ultrasonic. The coarse dendritic crystal is not beneficial to the rising of the bubbles and the melt feeding; however, the uniform and fine equiaxed crystals benefit from this. Therefore, when the best degassing effect is obtained, the solidification structure of the ingot often becomes fine and uniform.

4. Conclusions

Ultrasonic treatment can effectively remove the gas from the Mg-3.03Ca alloy, which can decrease the hydrogen content in the melt. Therefore, ultrasonic degassing is feasible in magnesium alloys, and the optimum degassing efficiency can be obtained under the ultrasonic resonant condition.

The effect of ultrasonic degassing is closely related to the ultrasonic treatment duration and treatment temperature. When applying ultrasonic treatment for 90 s with 150 W at 700 °C, the minimum hydrogen content and the highest degassing efficiency are obtained, respectively (42.8 cm³/100 g and 27.5%).

Ultrasonic treatment not only removes the gas from the melt but also uniformly refines the solidification structure, which is beneficial to the degassing effect.

Author Contributions: Z.J., data curation and writing—original draft. B.Y., investigation and validation. L.F., methodology. All authors have read and agreed to the published version of the manuscript.

Funding: The Key Project of the Education Department of Liaoning Province (Grant No. LJKZ1171), the China Postdoctoral Fund (2020M680978), and the Liaoning Province Doctor Start Fund Project (2020-BS-260).

Institutional Review Board Statement: Not applicable.

Informed Consent Statement: Not applicable.

Data Availability Statement: Not applicable.

Conflicts of Interest: The authors declare no conflict of interest.

References

1. Liu, J.; Sun, J.; Chen, Q.; Lu, L. Intergranular Cracking in Mg-Gd-Y Alloy during Tension Test. *Crystals* **2022**, *12*, 1040. [[CrossRef](#)]
2. Fu, T.; Sun, X.; Ge, C.; Xie, D.; Li, J.; Pan, H.; Qin, G. Achieving high strength-ductility synergy in dilute Mg-Al-Ca alloy by trace Ce addition. *J. Alloys Compd.* **2022**, *917*, 165407. [[CrossRef](#)]
3. Du, J.; Song, H.; An, M.; Li, Y. Effect of rare earth element on amorphization and deformation behavior of crystalline/amorphous dual-phase Mg alloys. *Mater. Des.* **2022**, *221*, 110979. [[CrossRef](#)]
4. Jin, Z.-Z.; Zha, M.; Wang, S.-Q.; Wang, S.-C.; Wang, C.; Jia, H.-L.; Wang, H.-Y. Alloying design and microstructural control strategies towards developing Mg alloys with enhanced ductility. *J. Magnes. Alloys* **2022**, *10*, 1191–1206. [[CrossRef](#)]
5. Rong, J.; Xiao, W.; Fu, Y.; Zhao, X.; Yan, P.; Ma, C.; Chen, M.; Huang, C. A high performance Mg–Al–Ca alloy processed by high pressure die casting: Microstructure, mechanical properties and thermal conductivity. *Mater. Sci. Eng. A* **2022**, *849*, 143500. [[CrossRef](#)]
6. Wang, C.; Dong, Z.; Li, K.; Sun, M.; Wu, J.; Wang, K.; Wu, G.; Ding, W. A novel process for grain refinement of Mg-RE alloys by low frequency electro-magnetic stirring assisted near-liquidus squeeze casting. *J. Mater. Process. Technol.* **2022**, *303*, 117537. [[CrossRef](#)]
7. Fu, J.; Xu, J.; Zhang, J.; Xu, G.; Li, Y.; Wang, Z. Effect of low cast-rolling speeds on the microstructure and mechanical properties of twin-roll casting high Mg AA5059 alloy sheets. *J. Mater. Res. Technol.* **2022**, *19*, 1059–1072. [[CrossRef](#)]
8. Liu, B.; Xu, K.; Zhang, Y.; Li, J. Hydrogen inhibition of sodium alginate and sodium phosphate on waste magnesium alloy dust particles: A new suppression method for magnesium alloy waste dust. *J. Loss Prev. Process Ind.* **2022**, *77*, 104753. [[CrossRef](#)]
9. Pang, X.; Ran, L.; Chen, Y.; Luo, Y.; Pan, F. Enhancing hydrogen storage performance via optimizing Y and Ni element in magnesium alloy. *J. Magnes. Alloys* **2021**, *10*, 821–835. [[CrossRef](#)]
10. Zheng, J.; Zhang, Z.; Le, Q.; Cui, J. Progress in Measuring Method to Hydrogen Content in Al and Mg Alloy. *Spec. Cast. Nonferrous Alloys* **2011**, *31*, 571–575.
11. Zhang, S.L.; Dong, X.W.; Zhao, Y.T.; Liu, M.P.; Gang, C.H.E.N.; Zhang, Z.K.; Zhang, Y.Y.; Gao, X.H. Preparation and wear properties of TiB₂/Al-30Si composites via in-situ melt reactions under high-energy ultrasonic field. *Trans. Nonferrous Met. Soc. China* **2014**, *24*, 3894–3900. [[CrossRef](#)]
12. Wang, A.; Gao, G.; Li, D.; Lu, D.; Wang, M.; Shi, D.; Xu, Z. A hollow exponential ultrasonic horn for aluminum melt degassing under power ultrasound and rotating flow field. *Results Phys.* **2021**, *21*, 103822. [[CrossRef](#)]

13. Jang, H.S.; Lee, G.H.; Jeon, J.B.; Choi, Y.S.; Shin, S. Effect of ultrasonic melt treatment conditions on melt quality of Al–Mg alloy. *J. Mater. Res. Technol.* **2022**, *19*, 2645–2656. [[CrossRef](#)]
14. Li, Z.; Xu, Z.; He, P.; Ma, Z.; Chen, S.; Yan, J. High speed imaging and numerical simulations of cavitation characteristic during the spreading of Galn melt under ultrasonication. *Int. J. Mech. Sci.* **2022**, *221*, 107221. [[CrossRef](#)]
15. Zhou, Z.; Wang, Q.; Chen, R.; Chen, D.; Zhao, T.; Su, Y. Solidification behavior and microstructure evolution of Nb-Si-Mo alloy in ultrasonic field. *Int. J. Refract. Met. Hard Mater.* **2022**, *108*, 105933. [[CrossRef](#)]
16. Chen, X.; Jia, Y.; Le, Q.; Ning, S.; Yin, Z.; Hu, C.; Yu, F. Understanding dual-frequency ultrasonic melt treatment on grain refinement and mechanical properties improvement of AZ80 magnesium alloy: Experiment and simulation. *J. Mater. Res. Technol.* **2021**, *15*, 4758–4767. [[CrossRef](#)]
17. Chen, H.; Guo, N.; Xu, K.; Xu, C.; Zhou, L.; Wang, G. In-situ observations of melt degassing and hydrogen removal enhanced by ultrasonics in underwater wet welding. *Mater. Des.* **2020**, *188*, 108482. [[CrossRef](#)]
18. Puga, H.; Barbosa, J.; Carneiro, V.; Barbosa, F.; Teixeira, J. Optimizing high-volume ultrasonic melt degassing using synchronized kinematic translation. *J. Mater. Res. Technol.* **2021**, *14*, 2832–2844. [[CrossRef](#)]
19. Abramov, O.V. *Ultrasound in Liquid and Solid Metals [M]*; CRC Press: Boca Raton, FL, USA, 1994.
20. Xu, H.; Meek, T.T.; Han, Q. Effects of ultrasonic field and vacuum on degassing of molten aluminum alloy. *Mater. Lett.* **2007**, *61*, 1246–1250. [[CrossRef](#)]
21. Xu, H.; Jian, X.; Meek, T.T.; Han, Q. Degassing of molten aluminum A356 alloy using ultrasonic vibration. *Mater. Lett.* **2004**, *58*, 3669–3673. [[CrossRef](#)]
22. Wu, S.; Liu, L.; Ma, Q.; Mao, Y.; An, P. Degassing effect of ultrasonic vibration in molten melt and semi-solid slurry of Al-Si alloys. *Chin. Foundry* **2012**, *9*, 201–206.
23. Wu, S.; Lü, S.; An, P.; Nakae, H. Microstructure and property of rheocasting aluminum-alloy made with indirect ultrasonic vibration process. *Mater. Lett.* **2012**, *73*, 150–153. [[CrossRef](#)]